Characterization of Some High-spin Iron(III) Complexes with Urea Derivatives. Crystal Structure of Diaquatetrakis(perhydropyrimidin-2-one)iron Trichloride Dihydrate and of Perhydropyrimidin-2-one

By **Sandro Calogero,*** Laboratorio di Chimica e Tecnologia dei Radioelementi del C.N.R., Corso Stati Uniti, 35100 Padova, Italy

Umberto Russo, Istituto di Chimica Generale ed Inorganica, Università di Padova, Via Loredan 4, 35100 Padova, Italy

Antonio Del Pra', Istituto di Chimica Organica, Università di Padova, Via Marzolo 1, 35100 Padova, Italy

High-spin complexes of the type $[FeL_6]X_3$, where L = urea, 1,3-dimethylurea (dmu), 1,3-diethylurea (deu), perhydropyrimidin-2-one (1,3-trimethyleneurea, tu), imidazolidin-2-one (1,3-ethyleneurea, eu), and X = ClO_4 or Br, and $[Fe(tu)_4(OH_2)_2]Cl_3\cdot 2H_2O$ have been prepared. A discrete octahedral geometry for all these complexes has been inferred from i.r., magnetic susceptibility, and Mössbauer measurements. The crystal structure of $[Fe(tu)_4(OH_2)_2]Cl_3\cdot 2H_2O$ has been solved by a three-dimensional Patterson synthesis: the crystals are orthorhombic, space group $P2_12_12_1$, with a = 18.627(9), b = 15.555(7), c = 9.876(5) Å, Z = 4, refined to R 0.056 for 2567 observable reflections. The iron atom is co-ordinated to two *cis*-oxygen atoms of two water molecules [Fe–O 2.028(5) and 2.036(5)Å respectively] and to four oxygen atoms of the tu ligands [Fe–O 1.996(5), 1.940(5), 1.995(5), and 2.000(5) Å respectively] in approximately octahedral manner. For comparison, the crystal structure of perhydropyrimidin-2-one has also been determined by direct methods: orthorhombic, space group *Pnam* (no. 62), with a = 10.282(3), b = 6.763(3), c = 7.171(2)Å, Z = 4, R 0.039, 392 observable reflections. Iterative extended-Hückel calculations have been performed.

SUBSTITUTED ureas are known to form many complexes with iron(III) having general formula FeL_nX_3 where n = 2, 3, or 6.[1-5] In most cases, a discrete structure with the ligands co-ordinated *via* the oxygen atom has been inferred from i.r. data while Mössbauer spectroscopy and magnetic susceptibility measurements point to an octahedral geometry and a high-spin electronic configuration. It seemed interesting to extend these studies to obtain further electronic and structural information, and so other complexes containing urea, 1,3-dimethylurea (dmu), 1,3-diethylurea (deu), perhydropyrimidin-2-one (1,3-trimethyleneurea, tu), imidazolidin-2-one (1,3-ethyleneurea, eu), and ClO_4, Cl, and Br have been prepared and characterized.

TABLE 1

Analytical data

Complex	M.p. [a] (θ$_c$/°C)	Λ [b] ohm^{-1} cm^2 mol^{-1}	$\mu_{eff.}$ B.M.	Analysis (%) [c] Fe		C		H		N		X	
(1) $[Fe(urea)_6][ClO_4]_3$	202	203.4	5.76	7.7	(7.8)	9.6	(10.1)	3.2	(3.4)	23.0	(23.5)	14.6	(14.9)
(2) $[Fe(dmu)_6][ClO_4]_3$	205	270.4	5.73	6.4	(6.3)	24.4	(24.5)	5.3	(5.5)	18.6	(19.0)	12.1	(12.1)
(3) $[Fe(deu)_6][ClO_4]_3$		288.6	5.95	5.6	(5.3)	33.2	(34.3)	6.6	(6.9)	15.5	(16.0)	10.8	(10.1)
(4) $[Fe(tu)_6][ClO_4]_3$	203	223.4	6.10	5.9	(5.9)	29.9	(30.2)	4.9	(5.1)	17.4	(17.6)	11.3	(11.1)
(5) $[Fe(eu)_6]Br_3$	137		5.50	7.0	(6.9)	27.5	(26.6)	4.6	(4.5)	26.7	(26.7)	28.7	(29.5)
(6) $[Fe(tu)_4(OH_2)_2]Cl_3\cdot 2\,H_2O$ [d]	152		6.02	8.7	(8.8)	29.6	(30.3)	6.4	(6.4)	17.6	(17.7)	17.6	(16.8)

1 B.M. ≈ 9.27×10^{-24} A m^2.

[a] Melting points were determined under vacuum and are uncorrected. [b] For 10^{-3} mol dm^{-3} solutions in $MeNO_2$ at 25 °C. [c] Calculated values are given in parentheses. [d] H_2O, 10.8 (11.4%)

The complexes, in particular with the tu ligand, show a great variety of stoicheiometry; besides the already reported complex $[Fe(tu)_4Cl_2][FeCl_4]$,[4] another, $Fe(tu)_3Cl_3$, was recently described.[3] Far-i.r. spectra support a discrete structure for the latter, while its Mössbauer spectrum indicates the presence of only one iron site. In this paper two new tu complexes are reported and the X-ray analysis of $[Fe(tu)_4(OH_2)_2]Cl_3\cdot 2H_2O$ has been performed. In order to study the effect of co-ordination of the tu molecule, the crystal structure of the free ligand has also been determined.

EXPERIMENTAL

Preparation of the Complexes.—All reagents were obtained from commercial sources and used without further purification. The solvents were purified before use according to standard methods. All the complexes were prepared in the same way;[3] as an example, the preparation of $[Fe(eu)_6]Br_3$ is reported. One gram of $FeBr_3$ was dissolved in few millilitres of acetone or ethanol; this solution was slowly poured into another in which the stoicheiometric quantity of the ligand was dissolved. The complex precipitated on addition of hexane or diethyl ether; it was washed with the solvent and dried under vacuum. Only $[Fe(tu)_4(OH_2)_2]Cl_3\cdot 2H_2O$ was obtained by slow evaporation of the solvent in the atmosphere. All of the complexes were recrystallized to constant analysis and identified by i.r. spectroscopy. The products were crystalline materials, stable in the solid state. Elemental analyses and melting points are reported in Table 1 together with the water content determined by the Karl Fisher method. The iron percentage was determined by atomic absorption spectroscopy using a Perkin-Elmer 300 instrument. The crystal of perhydropyrimidin-2-one used for the X-ray study was obtained as a transparent prism by slow evaporation from acetone.

Magnetic susceptibilities were determined at room temperature by the Gouy method; the magnetic balance was calibrated with $[Ni(en)_3][S_2O_3]$ (en = ethylenediamine) and

Pascal's constants were used to correct for diamagnetism. Conductivity data were obtained on an LKB type 3216 B bridge at room temperature in a conventional closed cell, using 10^{-3} mol dm^{-3} solutions in $MeNO_2$. Conductivity and magnetic data are also reported in Table 1. Infrared spectra were recorded on Beckman IR 9 and Perkin-Elmer 850 instruments using KBr pellets, far-i.r. spectra as Nujol mulls on a Beckman IR 11 spectrophotometer. Some relevant i.r. bands are listed in Table 2.

TABLE 2

Some relevant i.r. bands (cm^{-1})

Mode	Ligand	Complex	
	urea [a]	$[Fe(urea)_6][ClO_4]_3$	
ν(CO)	1 686	1 631	
ν(CN)	1 468	1 503	
	dmu [b]	$[Fe(dmu)_6][ClO_4]_3$	
ν(CO)	1 635	1 587	
ν(CN)	1 410	1 448	
	deu [c]	$[Fe(deu)_6][ClO_4]_3$	
ν(CO)	1 645	1 585	
	tu [d]	$[Fe(tu)_6]$-$[ClO_4]_3$	$[Fe(tu)_4(OH_2)_2]$-$Cl_3 \cdot 2H_2O$
ν(CO)	1 686	1 630	1 614
δ(NH)	1 540	1 590	1 581
ν(NH)	1 316	1 322	1 318
ρ(NH)	782	843	844
	eu [e]	$[Fe(eu)_6]Br_3$	
ν(CO)	1 660	1 633	
δ(NH)	1 502	1 534	
ρ(NH)	700	745	

[a] See ref. 16. [b] See ref. 1. [c] See ref. 17. [d] See ref. 4. [e] See ref. 5.

Crystal and Intensity Data.—Diaquatetrakis(perhydropyrimidin-2-one)iron trichloride dihydrate, $[Fe(tu)_4(OH_2)_2]Cl_3 \cdot 2H_2O$. $C_{16}H_{40}Cl_3FeN_8O_8$, $M = 634.76$, Orthorhombic, $a = 18.627(9)$, $b = 15.555(7)$, $c = 9.876(5)$ Å, $U = 2\,861.5(4)$ Å^3, $D_m = 1.46$ (by flotation), $Z = 4$, $D_c = 1.47$ g cm^{-3}, $F(000) = 1\,236$, $\lambda(\text{Mo-}K_\alpha) = 0.710\,69$ Å, $\mu(\text{Mo-}K_\alpha) = 8.57$ cm^{-1}, space group $P2_12_12_1$, crystal dimensions $0.35 \times 0.20 \times 0.70$ mm.

Intensity data were collected using a Philips PW 1100 four-circle diffractometer in the range $4 \leqslant 2\theta \leqslant 50°$, with Mo-$K_\alpha$ radiation (graphite monochromator, θ—2θ scan mode, scan width 1.2°, scan speed 0.03° s^{-1}). Three standard reflections were measured every 120 min. Using the criterion $I \geqslant 3\sigma(I)$, 2 567 of the 2 845 recorded intensities were independent and observable. The data were corrected for Lorentz and polarization effects, and for absorption following the method proposed by North *et al.*[6]

TABLE 3

Final fractional atomic co-ordinates for $[Fe(tu)_4(OH_2)_2]Cl_3 \cdot 2H_2O$ with estimated standard deviations in parentheses

Atom	x/a	y/b	z/c
Fe	0.154 8(1)	0.233 7(1)	0.358 5(1)
Cl(1)	0.412 0(1)	0.226 0(2)	0.160 2(3)
Cl(2)	0.032 9(1)	0.483 0(2)	0.378 0(3)
Cl(3)	0.182 2(1)	0.312 7(2)	−0.067 1(2)
O(1)	0.204 3(3)	0.208 5(4)	0.533 3(5)
O(2)	0.226 7(3)	0.163 5(4)	0.257 5(6)
O(3)	0.214 4(3)	0.335 2(4)	0.339 2(6)
O(4)	0.079 5(3)	0.302 3(4)	0.461 7(6)
O(5)	0.090 8(3)	0.130 9(3)	0.373 0(6)
O(6)	0.102 1(3)	0.265 1(4)	0.185 7(5)
O(7)	0.066 1(4)	0.281 9(7)	0.718 9(6)
O(8)	−0.002 5(4)	0.178 3(5)	0.071 7(8)
N(1)	0.281 8(4)	0.238 5(6)	0.699 5(7)
N(2)	0.323 8(3)	0.208 8(5)	0.483 9(7)
N(3)	0.298 7(4)	0.382 1(5)	0.194 0(8)
N(4)	0.194 8(4)	0.457 9(5)	0.227 9(9)
N(5)	0.280 7(4)	0.103 8(5)	0.078 2(7)
N(6)	0.162 5(4)	0.072 8(4)	0.124 7(7)
N(7)	0.019 1(4)	0.020 4(5)	0.423 9(8)
N(8)	0.066 7(4)	0.103 4(6)	0.594 1(7)
C(1)	0.269 0(4)	0.218 8(6)	0.569 7(9)
C(2)	0.398 8(6)	0.221 1(7)	0.524 0(11)
C(3)	0.405 6(9)	0.201 1(11)	0.680 0(18)
C(31)	0.408 2(20)	0.274 0(25)	0.633 1(43)
C(4)	0.353 4(6)	0.251 4(7)	0.755 6(10)
C(5)	0.234 8(4)	0.390 8(5)	0.252 8(9)
C(6)	0.326 0(6)	0.441 3(7)	0.094 4(11)
C(7)	0.297 3(6)	0.529 0(8)	0.121 5(13)
C(8)	0.215 4(6)	0.525 0(8)	0.130 5(14)
C(9)	0.222 6(4)	0.115 1(5)	0.152 4(9)
C(10)	0.278 4(7)	0.048 9(8)	−0.045 6(13)
C(11)	0.205 8(7)	0.048 9(9)	−0.102 2(14)
C(12)	0.152 2(6)	0.021 4(7)	0.001 4(11)
C(13)	0.058 9(4)	0.086 3(5)	0.462 3(9)
C(14)	−0.018 9(6)	−0.036 0(8)	0.516 2(12)
C(15)	−0.033 8(8)	0.007 6(9)	0.641 1(17)
C(16)	0.029 2(8)	0.051 7(9)	0.699 2(14)
H(1) [a]	0.236	0.247	0.767
H(2)	0.312	0.191	0.380
H(3)	0.330	0.330	0.226
H(4)	0.143	0.437	0.282
H(5)	0.331	0.135	0.108
H(6)	0.118	0.077	0.195
H(7)	0.014	0.010	0.316
H(8)	0.104	0.156	0.622
H(21)	0.434	0.179	0.465
H(22)	0.415	0.288	0.502
H(31)	0.458	0.218	0.708
H(32)	0.395	0.135	0.689
H(41)	0.366	0.319	0.755
H(42)	0.353	0.228	0.859
H(61)	0.384	0.442	0.099
H(62)	0.310	0.420	0.994
H(71)	0.318	0.552	0.217
H(72)	0.313	0.572	0.041
H(81)	0.193	0.514	0.032
H(82)	0.196	0.588	0.167
H(101)	0.319	0.076	0.958
H(102)	0.298	0.986	0.986
H(111)	0.203	0.003	0.813
H(112)	0.191	0.112	0.860
H(121)	0.162	0.954	0.026
H(122)	0.099	0.029	0.964
H(141)	0.013	0.908	0.535
H(142)	0.931	0.945	0.469
H(151)	0.926	0.055	0.621
H(152)	0.947	0.960	0.711
H(161)	0.014	0.089	0.781
H(162)	0.067	0.000	0.783
H(104) [b]	0.078	0.363	0.437
H(204) [b]	0.038	0.320	0.488
H(106) [b]	0.124	0.279	0.109
H(206) [b]	0.063	0.241	0.158
H(107) [b]	0.524	0.207	0.242
H(207) [b]	0.600	0.219	0.224
H(108) [b]	0.983	0.118	0.093
H(208) [b]	0.017	0.192	0.002

[a] All hydrogen-atom co-ordinates were calculated. [b] Found on ΔF map, but not refined.

Perhydropyrimidin-2-one, tu. $C_4H_8N_2O$, $M = 100.12$, Orthorhombic, $a = 10.282(3)$, $b = 6.763(3)$, $c = 7.171(2)$ Å, $U = 498.6(5)$ Å^3, $D_m = 1.32$ (by flotation), $Z = 4$, $D_c = 1.33$ g cm^{-3}, $F(000) = 216$, $\lambda(\text{Mo-}K_\alpha) = 0.710\,69$ Å, $\mu(\text{Mo-}K_\alpha) = 0.92$ cm^{-1}, space group *Pnam* (no. 62), crystal dimensions $0.50 \times 0.30 \times 0.10$ mm.

Intensity data were collected as for the complex. Among the 475 reflections, 392 were considered observable according to the criterion $I \geqslant 3\sigma(I)$. Corrections were made for Lorentz-polarization, but not for the effects of *X*-ray absorption.

TABLE 4

Bond distances (Å) and angles (°) for $[Fe(tu)_4(OH_2)_2]Cl_3{\cdot}2H_2O$ with estimated standard deviations in parentheses

(*a*) Distances

Fe–O(1)	1.996(5)	Fe–O(2)	1.995(5)	Fe–O(3)	1.940(5)	Fe–O(5)	2.000(5)	Fe–O(4)	2.036(5)
O(1)–C(1)	1.268(9)	O(2)–C(9)	1.285(9)	O(3)–C(5)	1.272(9)	O(5)–C(13)	1.269(9)	O(4)–H(104)	0.98(1)
C(1)–N(1)	1.340(10)	C(9)–N(5)	1.319(10)	C(5)–N(3)	1.332(10)	C(13)–N(7)	1.321(10)	O(4)–H(204)	0.85(1)
N(1)–C(4)	1.459(11)	N(5)–C(10)	1.492(13)	N(3)–C(6)	1.440(11)	N(7)–C(14)	1.449(12)	Fe–O(6)	2.028(5)
C(4)–C(3)	1.454(18)	C(10)–C(11)	1.464(15)	C(6)–C(7)	1.490(14)	C(14)–C(15)	1.436(17)	O(6)–H(106)	0.89(1)
C(3)–C(2)	1.576(19)	C(11)–C(12)	1.491(15)	C(7)–C(8)	1.530(14)	C(15)–C(16)	1.476(17)	O(6)–H(206)	0.87(1)
C(2)–N(2)	1.466(11)	C(12)–N(6)	1.470(12)	C(8)–N(4)	1.470(14)	C(16)–N(8)	1.487(14)	C(4)–C(31)	1.622(38)
N(2)–C(1)	1.336(10)	N(6)–C(9)	1.327(10)	N(4)–C(5)	1.306(10)	N(8)–C(13)	1.336(10)	C(31)–C(2)	1.367(39)
								C(31)–C(3)	1.225(37)

(*b*) Angles

O(1)–Fe–O(2)	90.8(0.2)	Fe–O(1)–C(1)	131.2(0.5)	Fe–O(2)–C(9)	133.2(0.5)
O(2)–Fe–O(3)	90.7(0.2)	O(1)–C(1)–N(1)	118.0(0.7)	O(2)–C(9)–N(5)	118.6(0.7)
O(3)–Fe–O(4)	91.0(0.2)	C(1)–N(1)–C(4)	123.9(0.7)	C(9)–N(5)–C(10)	120.6(0.8)
O(4)–Fe–O(5)	88.4(0.2)	N(1)–C(4)–C(3)	110.0(0.9)	N(5)–C(10)–C(11)	109.8(1.0)
O(2)–Fe–O(6)	92.0(0.2)	C(4)–C(3)–C(2)	110.2(1.2)	C(10)–C(11)–C(12)	110.9(1.1)
O(1)–Fe–O(4)	89.3(0.2)	C(3)–C(2)–N(2)	108.4(0.9)	C(11)–C(12)–N(6)	109.0(0.9)
O(1)–Fe–O(5)	93.2(0.2)	C(2)–N(2)–C(1)	122.8(0.7)	C(12)–N(6)–C(9)	123.4(0.7)
O(1)–Fe–O(3)	88.9(0.2)	N(2)–C(1)–O(1)	122.1(0.7)	N(6)–C(9)–O(2)	120.5(0.7)
O(3)–Fe–O(6)	89.9(0.2)	N(1)–C(1)–N(2)	119.9(0.7)	N(5)–C(9)–N(6)	120.8(0.7)
Fe–O(3)–C(5)	142.1(0.5)	Fe–O(5)–C(13)	139.9(0.5)	Fe–O(4)–H(104)	113.7(5.5)
O(3)–C(5)–N(3)	119.4(0.8)	O(5)–C(13)–N(7)	119.1(0.7)	Fe–O(4)–H(204)	159.9(0.5)
C(5)–N(3)–C(6)	123.3(0.8)	C(13)–N(7)–C(14)	124.3(0.8)	H(104)–O(4)–H(204)	74.6(5.4)
N(3)–C(6)–C(7)	109.6(0.8)	N(7)–C(14)–C(15)	110.4(1.0)	Fe–O(6)–H(106)	123.6(0.4)
C(6)–C(7)–C(8)	109.3(1.0)	C(14)–C(15)–C(16)	113.6(1.2)	Fe–O(6)–H(206)	124.3(0.5)
C(7)–C(8)–N(4)	109.1(1.0)	C(15)–C(16)–N(8)	110.7(1.1)	H(106)–O(6)–H(206)	103.1(0.5)
C(8)–N(4)–C(5)	122.8(0.8)	C(16)–N(8)–C(13)	121.5(0.9)	N(1)–C(4)–C(31)	108.8(1.4)
N(4)–C(5)–O(3)	120.0(0.8)	N(8)–C(13)–O(5)	121.2(0.7)	C(4)–C(31)–C(2)	112.1(2.3)
N(3)–C(5)–N(4)	120.6(0.8)	N(7)–C(13)–N(8)	119.6(0.8)	C(31)–C(2)–N(2)	114.5(1.7)

Solution and Refinement of the Structures.—The molecular structure of $[Fe(tu)_4(OH_2)_2]Cl_3{\cdot}2H_2O$ was solved by difference electron-density syntheses following successful location of the Fe and Cl atoms from a three-dimensional Patterson synthesis. A full-matrix least-squares refinement of F was computed, minimizing the function $\Sigma w(|F_o| - |F_c|)^2$ where $w = 1$. Throughout the analysis, the scattering factors of ref. 7 were used, and both the real and imaginary components of anomalous dispersion were included for Fe and Cl.[8] The Fe, Cl, O, and N atoms were refined aniso-

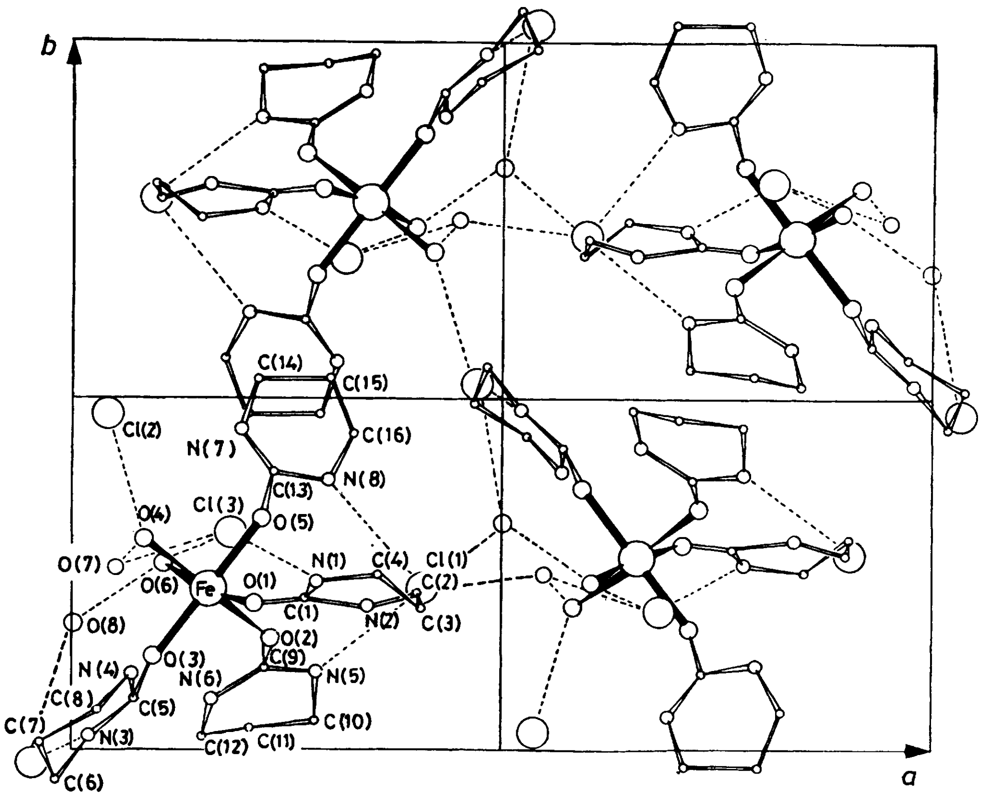

FIGURE 1 Perspective of $[Fe(tu)_4(OH_2)_2]Cl_3{\cdot}2H_2O$ with atom-numbering scheme and crystal packing

tropically, while isotropic thermal parameters were assigned to the C atoms. A C–H distance of 1.08 Å was employed. For the 2 567 observed reflections the final conventional R value was 0.056. The stereochemical arrangement of the complex is shown in Figure 1, together with the atom-numbering scheme. The final atomic co-ordinates with their standard deviations are listed in Table 3, bond distances and angles, uncorrected for changes due to thermal vibrations, in Table 4, and some interatomic distances in Table 5.

TABLE 5

Interatomic distances less than 3.4 Å for $[Fe(tu)_4(OH_2)_2]Cl_3 \cdot 2H_2O$

O(7)–Cl(1^{I})	3.111 *	O(8)–Cl(2)	2.130 *
O(7)–Cl(3^{I})	3.062 *	O(6)–Cl(3)	3.001 *
N(1)–Cl(3^{I})	3.176 *	O(7)–O(1)	3.360
O(8)–Cl(1)	3.162 *	O(4)–Cl(2^{II})	3.056 *
N(7)–Cl(2)	3.188 *	N(4)–Cl(2^{II})	3.383
O(7)–O(4)	2.572 *	C(2)–O(4^{III})	3.388
O(8)–O(6)	2.624 *	C(4)–O(8^{III})	3.363
O(7)–N(8)	3.038 *	N(5)–Cl(^{IV})	3.202 *
		N(3)–Cl(1^{IV})	3.234 *

Symmetry operators: I, $x, y, 1 + z$; II, $\bar{x}, \frac{1}{2} + y, \frac{1}{2} - z$; III, $\frac{1}{2} + x, \frac{1}{2} - y, 1 - z$; IV, $\frac{1}{2} + x, \frac{1}{2} - y, \bar{z}$

* Possible hydrogen bond.

The molecular structure of perhydropyrimidin-2-one (tu) was solved by direct methods using non-centrosymmetric phase relations. Normalized structure factors were calculated and the 178 reflections with $|E(hkl)| \geqslant 1.02$ were used in the phasing program MULTAN.[9] The E map showed the tu molecule to lie on the mirror plane of the centrosymmetric space group. The refinement of the structure parameters was carried out by full-matrix least-squares analysis, allowing the non-hydrogen atoms to vibrate anisotropically. All the hydrogen atoms were located from difference-Fourier maps and then included in the refinement with isotropic thermal parameters equivalent to the anisotropic ones of the atoms to which the hydrogens are bound.[10] The function $\Sigma w(|F_o| - |F_c|)^2$, where $w = 1$, was minimized and the final R value for the 392 observed reflections was 0.039. The ΔF map showed a high electron density corresponding to an alternate site of the apical carbon atom C(3), and so a new carbon atom, C(31), was inserted. The occupance ratio C(3) : C(31) = 0.7 : 0.3 was determined with fixed thermal parameters; these were free only in the successive least-squares cycles. The atomic scattering factors used for all the atoms were obtained from ref. 7. A perspective view of the tu molecule is shown in Figure 2. The fractional co-ordinates, bond distances, bond and torsion angles with their standard deviations are reported in Table 6.

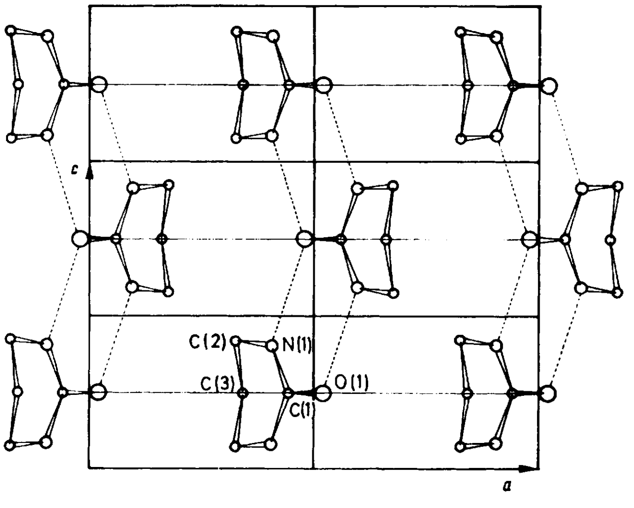

FIGURE 2 Perspective of perhydropyrimidin-2-one (tu) with atom-numbering scheme and crystal packing

Observed and calculated structure factors for $[Fe(tu)_4(OH_2)_2]Cl_3 \cdot 2H_2O$ and for perhydropyrimidin-2-one, together with their anisotropic thermal parameters, are listed in Supplementary Publication No. SUP 22702 (28 pp.).*

TABLE 6

Final fractional atomic co-ordinates, bond distances (Å), and torsion angles (°) for perhydropyrimidin-2-one with estimated standard deviations in parentheses

(*a*) Final fractional atomic co-ordinates

Atom	x/a	y/b	z/c
O(1)	0.516 5(5)	0.481 1(8)	0.250 0
N(1)	0.414 2(4)	0.722 4(7)	0.410 9(6)
C(1)	0.449 4(7)	0.636 2(11)	0.250 0
C(2)	0.329 5(6)	0.896 0(9)	0.422 2(9)
C(3)	0.346 4(9)	1.021 7(13)	0.250 0
H(N)	0.434(6)	0.659(9)	0.518(10)
H(21)	0.353(6)	0.966(10)	0.546(9)
H(22)	0.231(7)	0.853(9)	0.434(9)
H(31)	0.439(9)	1.088(14)	0.250
H(32)	0.280(9)	1.128(14)	0.250

(*b*) Distances

O(1)–C(1)	1.256(4)	C(2)–H(21)	1.03(3)
C(1)–N(1)	1.342(2)	C(2)–H(22)	1.06(3)
N(1)–C(2)	1.464(3)	C(3)–H(31)	1.05(4)
C(2)–C(3)	1.509(3)	C(3)–H(32)	0.99(4)
		N(1)–H(N)	0.90(4)

(*c*) Angles

O(1)–C(1)–N(1)	120.7(0.1)	H(21)–C(2)–H(22)	106.4(2.1)
N(1)–C(1)–N(1′)	118.5(0.2)	H(22)–C(2)–C(3)	109.4(1.6)
C(1)–N(1)–C(2)	123.8(0.2)	H(21)–C(2)–C(3)	114.5(1.5)
H(N)–N(1)–C(1)	117.9(1.1)	H(22)–C(2)–N(1)	110.6(1.6)
H(N)–N(1)–C(2)	117.7(1.2)	C(2)–C(3)–C(2′)	109.8(0.3)
N(1)–C(2)–C(3)	109.8(0.2)	H(31)–C(3)–C(2)	110.1(1.1)
N(1)–C(2)–H(21)	106.2(1.5)	H(32)–C(3)–C(2)	109.4(1.1)
		H(31)–C(3)–H(32)	108.1(3.0)

(*d*) Torsion angles *

N(1′)–C(1)–N(1)–C(2)	−5.7
C(1)–N(1)–C(2)–C(3)	30.0
N(1)–C(2)–C(3)–C(2′)	−52.2

* The torsion angle of the bonded group A–X–Y–B is the angle between the planes A–X–Y and X–Y–B, positive if clockwise and negative if counterclockwise.

Mössbauer Parameters.—Mössbauer spectra were recorded on a conventional constant-acceleration spectrometer using a 50-mCi $^{57}Co(Rh)$ source at room temperature. Calibration was effected using α-iron but the isomer-shift values are relative to sodium nitroprusside for direct comparison purposes with the previous literature. The data points were fitted to Lorentzian lineshapes by an iterative least-squares program. A typical Mössbauer spectrum at various temperatures, together with the calculated curves, is shown in Figure 3. Table 7 lists the Mössbauer isomer shifts (δ) and the full widths at half-weight (Γ).

Iterative extended Hückel-method (IEHM) calculations were carried out by a FORTRAN program developed to

---

* For details see Notices to Authors No. 7, *J.C.S. Dalton*, 1979, Index issue.

handle a very large set of atomic orbitals. In all calculations the basis set was limited to valence electrons; the Slater exponents [11] and valence-orbital ionization potentials [12] were derived from the literature, and the Wolfsberg–Helmholtz approximation was used. The crystallographic data of $[Fe(tu)_4(OH_2)_2]Cl_3{\cdot}2H_2O$ and tu were used as input. A Mulliken population analysis [13] was performed. The lattice and valence contributions to the quadrupole splitting were calculated using already reported methods and values.[14] Table 9 lists some results of the semi-empirical IEHM calculations.

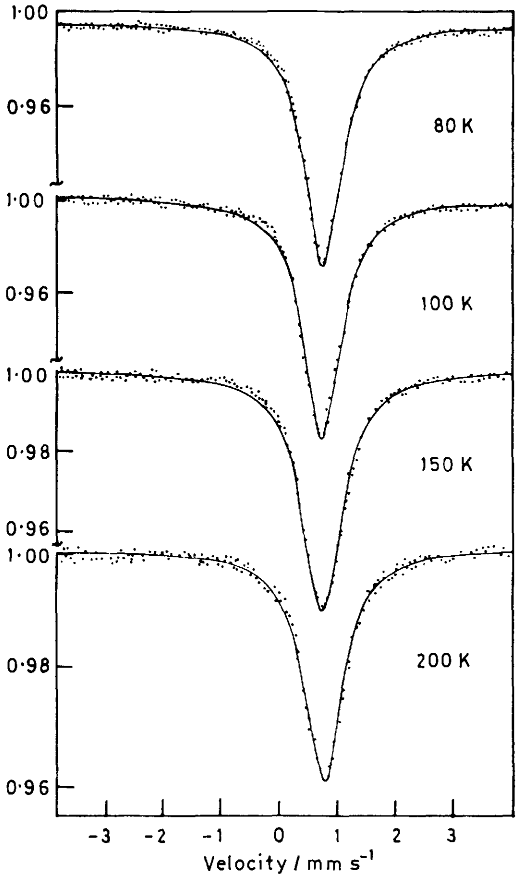

FIGURE 3 Mössbauer spectra of $[Fe(tu)_4(OH_2)_2]Cl_3{\cdot}2H_2O$ at various temperatures showing the experimental points and calculated curves

TABLE 7

Mössbauer parameters (δ and Γ in mm s^{-1})

Complex	T/K	δ [a]	Γ [b]
(1)	295	0.61	0.90
(2)	295	0.58	0.94
(3)	295	0.61	0.92
(4)	80	0.59	0.96
(5)	295	0.55	0.98
(6) [c]	80	0.67	0.90

[a] Relative to sodium nitroprusside; the accuracy is ±0.03 mm s^{-1}. [b] The accuracy is ±0.01 mm s^{-1}. [c] No observed Mössbauer effect at room temperature.

The SHELX-76 system of crystallographic programs,[15] the Mössbauer fitting program, and the IEHM program were used on a CDC Cyber 76 computer.

RESULTS AND DISCUSSION

General Comments.—The i.r. data of Table 2 show that urea,[16] 1,3-dimethylurea,[1] 1,3-diethylurea,[17] perhydropyrimidin-2-one,[4] and imidazolidin-2-one [5] are co-ordinated to iron through their oxygen atoms. The C–N stretching frequency shows a positive shift on going from the free to the co-ordinated ligand, while the C=O stretching has a negative shift because of the weakening of the double bond on formation of a Fe–O bond. This shift shows interesting variations in the complexes with the tu ligand: thus, while $[Fe(tu)_6][ClO_4]_3$ and $Fe(tu)_3Cl_3$ [3] give similar values for the ν(C=O) band (1 630 and 1 626 cm^{-1} respectively), $[Fe(tu)_4(OH_2)_2]Cl_3{\cdot}2H_2O$ shows an anomalous shift (1 614 cm^{-1}), suggesting a significant influence of the water content in the co-ordination sphere of the complex. This influence was explained by the X-ray study which shows a discrete structure with two water molecules completing the co-ordination sphere of the iron.

The presence of two i.r. bands due to unco-ordinated perchlorate ion at 1 030—1 200 and 630 cm^{-1} in the spectra of complexes (1)—(4) of Table 1 points to a discrete ionic structure.[18] This statement agrees with the conductivity data, which indicate an ionic (1 : 3) nature for these complexes. Also for complexes (5) and (6) of Table 1, the far-i.r. data suggest a discrete ionic structure; in fact the spectra do not show any absorption due to terminal or bridging Fe–Br or Fe–Cl bonds. Such an assignment for all our complexes agrees with the monomeric structure already proposed for $[Fe(urea)_6]Cl_3$, $[Fe(urea)_6]Br_3$, $[Fe(tu)_6]Br_3$, and $Fe(tu)_3Cl_3$.[3]

TABLE 8

Least-squares planes in $[Fe(tu)_4(OH_2)_2]Cl_3{\cdot}2H_2O$ and tu in the form $AX + BY + CZ + D = 0$ with deviations (Å) from the plane in square brackets

(*a*) $[Fe(tu)_4(OH_2)_2]Cl_3{\cdot}2H_2O$

Plane (I): $A = 0.449\,1$, $B = -0.234\,9$, $C = 0.862\,1$, $D = 3.477\,9$
[Fe 0.015, O(2) 0.013, O(3) −0.021, O(4) 0.013, O(5) −0.021]

Plane (II): $A = 0.670\,4$, $B = -0.539\,0$, $C = -0.510\,0$, $D = -1.856\,0$
[Fe 0.024, O(1) −0.027, O(3) 0.015, O(5) 0.014, O(6) −0.027]

Plane (III): $A = 0.566\,8$, $B = 0.817\,2$, $C = -0.104\,6$, $D = 4.231\,4$
[Fe 0.003, O(1) 0.025, O(2) −0.026, O(4) −0.027, O(6) 0.024]

Plane (IV): $A = 0.484\,9$, $B = 0.515\,2$, $C = 0.735\,4$, $D = 6.905\,2$
[O(3) 0.000, C(5) −0.016, N(3) 0.017, N(4) 0.005, C(6) −0.009, C(7) * 0.647, C(8) 0.002]

(*b*) tu

Plane (V): $A = 0.833\,6$, $B = 0.552\,4$, $C = 0.000\,0$, $D = 6.203\,0$
[O(1) −0.054, C(1) 0.025, N(1) 0.046, N(1′) 0.046, C(2) −0.032, C(2′) −0.032, C(3) * 0.583]

Plane (VI): $A = 0.859\,3$, $B = 0.511\,5$, $C = 0.000\,0$, $D = 6.161\,6$
[O(1) −0.003, C(1) 0.010, N(1) −0.003, N(1′) −0.003, C(2) * − 0.151, C(2′) * − 0.151, C(3) * 0.433]

*Atom not used in the calculations.

The values of the magnetic moments at room temperature indicate a high-spin electronic configuration for all the reported complexes, and is confirmed by the Mössbauer isomer-shift values of Table 7 which are within the range normally observed for octahedral high-spin iron(III) complexes.[19]

Crystal Structure of Diaquatetrakis(perhydropyrimidin-2-one)iron Trichloride Dihydrate.—The crystal structure of the complex consists of discrete $[Fe(tu)_4(OH_2)_2]^{3+}$ cations, chlorine anions, and water molecules of crystallization. The geometry of the cation is octahedral: three oxygens of tu and one of water occupy the equatorial plane, and two other oxygens, one from tu and one from a water molecule, complete the co-ordination sphere around the iron (Figure 3). The deviations of the atoms from the least-squares planes (I)—(III) of Table 8 and the bond angles and distances (Table 4) show a nearly regular octahedral geometry around the iron atom, in agreement with the lack of a quadrupole splitting of its Mössbauer spectrum (Figure 3). The bond distances Fe–O(1), Fe–O(2), and Fe–O(5) are very similar, while Fe–O(3) is *ca.* 0.057 Å shorter. On the other hand, the distances Fe–O(4) and Fe–O(6) are significantly longer than these values, indicating that most of the negative charge resides on the amide oxygen atoms. As shown in Table 9, the amide oxygen atoms possess a charge of *ca.* —0.41 compared with *ca.* —0.21 on the water oxygen atoms. Nevertheless all Fe–O distances in the complex generally fall within the range usually found.[20-24] As expected, the distances between the iron and the oxygen atom of the water of crystallization are very large: Fe–O(7) 3.995 and Fe–O(8) 4.165 Å.

TABLE 9

Some significant atomic charge values for $[Fe(tu)_4(OH_2)_2]^{3+}$, $[Fe(tu)_6]^{3+}$, and tu

Compound	Atom	Charge	Atom	Charge	Atom	Charge
$[Fe(tu)_4(OH_2)_2]^{3+}$ [a]	Fe	−0.13				
	O(1)	−0.41	C(1)	0.17		
	O(2)	−0.41	C(9)	0.17		
	O(3)	−0.42	C(5)	0.16		
	O(4)	−0.22	H(104)	0.12	H(204)	0.14
	O(5)	−0.39	C(13)	0.16		
	O(6)	−0.19	H(106)	0.11	H(206)	0.11
$[Fe(tu)_6]^{3+}$ [b]	Fe	-0.12_5				
	O(1)	−0.39	C(1)	0.18		
	O(2)	−0.39	C(9)	0.18		
	O(3)	−0.40	C(5)	0.18		
	O(2′) [c]	−0.40	C(9′) [c]	0.18		
	O(5)	−0.39	C(13)	0.17		
	O(1′) [c]	−0.39	C(1′) [c]	0.17		
tu [d]	O(1)	−0.14	H(N)	0.09		
	N(1)	−0.12	H(21)	0.03		
	C(1)	0.17	H(22)	0.03		
	C(2)	0.07	H(31)	0.02		
	C(3)	0.03	H(32)	0.03		

[a] *Cf.* Figure 1 for the atom-numbering scheme. [b] The crystal data for $[Fe(tu)_4(OH_2)_2]^{3+}$ were used but two tu groups were substituted for the water molecules. [c] Primed atoms correspond to the atoms of the two tu ligands after inversion with respect to iron. [d] *Cf.* Figure 2 for the atom-numbering scheme.

As is usually observed in other urea complexes, the iron–oxygen–carbon angles are higher than the ideal trigonal value. This may be due to steric hindrance of the amino-groups bound to the carbon atom.

For comparison, only the plane of the atoms O(3), C(5), N(3), C(6), C(8), and N(4) of the tu ligand is reported. For this [plane (IV) in Table 8], which is by far the worst least-squares plane, the maximum deviation is 0.017 Å.

A complex network of hydrogen bonding contributes to the cohesion of the structure. The crystal packing is mainly determined by O–H ··· Cl and N–H ··· Cl bonds, as shown in Figure 1 and Table 5 where only interatomic distances less than 3.4 Å are reported. It is also interesting to note that only one nitrogen atom for each tu ligand is involved in hydrogen bonds with Cl anions. The chlorine anions are co-ordinated through hydrogen bonds to two water molecules: Cl(1) to two water molecules of crystallization, Cl(2) and Cl(3) to one water molecule of crystallization and one of the co-ordination sphere. The very long Fe–Cl distances, 5.177, 4.498, and 4.409 Å respectively, agree with the absence of Fe–Cl far-i.r. bands.

The effect of co-ordination of perhydropyrimidin-2-one through its oxygen atom (Table 2) may be observed by comparing the C–O bond length and bond order in the complex and in the free molecule. To study this effect, the crystal structure of the free tu was determined.

Crystal Structure of Perhydropyrimidin-2-one (*tu*).—A perspective view of the title compound showing its conformation and the atom-numbering scheme is shown in Figure 2. The bond angles around carbon atom C(1) correspond to trigonal hybridization; the bond distances indicate 60% double-bond character for the C–O bond and 20% for each C–N bond.[25] The electronic structure of the urea derivatives may be represented as a suitably weighted hybrid of ionic and covalent forms; the atomic charges —0.41 on O(1), 0.17 on C(1), and —0.12 on N(1) (Table 9) were calculated for the tu molecule.

It is expected that co-ordination *via* oxygen should decrease the bond order and increase the bond length, enhancing the contribution of ionic forms. The C–O bond length in tu is 1.256(4) Å while in $[Fe(tu)_4(OH_2)_2]$-

$Cl_3\cdot 2H_2O$ it ranges from 1.268(9) to 1.285(9) Å (mean 1.274 Å). This very small difference ($<3\sigma$) is probably insignificant, but the C–O stretching values of Table 2 show that there is indeed a small effect of this type. The trend seems to be confirmed, also, by the bond-order values: the C–O bond order in the tu ligand, 0.78, decreases to an average value of 0.71 in the complex. Apart from this case, on going from free to bound tu (Tables 4 and 6), the bond distances and angles show no large variations.

The bond angles around carbon atoms C(2) and C(3) are very close to those of a regular tetrahedron. It is therefore reasonable to consider the observed C(2)–C(3) bond length (1.509 Å) as single even if it is 0.031 Å shorter than the accepted length; similar values have already been found in trimethylenethiourea.[25]

Both the C(1)–N(1)–C(2) bond angle and the N(1)–H(N) bond length indicate that the nitrogen atom is trigonally hybridized. The N(1)–C(2) distance represents a single bond even if shorter than the sum of the appropriate covalent radii, 1.47 Å. The amide bond lengths and angles are in good agreement with those of urea,[26] monomethylurea,[27] and other similar molecules.[28]

Among the intermolecular distances, only that between O(1) and N(1) $(1 - x, 1 - y, 1 - z)$ (2.883 Å) is less than 3.5 Å as shown in Figure 2, where the separation among molecules related by the mirror plane and glide plane is also presented. This distance is characteristic for $O \cdots N$ hydrogen bonds and further support for this interpretation is the $H(N) \cdots O''$ distance (1.74 Å), which is much smaller than the sum of the van der Waals radii. As usual in hydrogen-bonded structures, the hydrogen atom does not lie directly on the $O \cdots N$ line, with the result that the $O'' \cdots H–N$ angle is 64.2°. Each nitrogen atom has one hydrogen bond, while each oxygen atom takes part in two hydrogen bonds and these, with the O–C bond, form a pyramidal arrangement. In contrast to the complex (Figure 1), where only one nitrogen atom from each tu molecule is involved in hydrogen bonding, both the nitrogen atoms of the free ligand are involved in hydrogen bonds (Figure 2).

Some least-squares planes for tu are reported in Table 8: the atoms O(1), C(1), N(1), C(2), N(1′), and C(2′) are coplanar, as is observed for the corresponding atoms of the tu ligand in the complex. The plane of the amide group O(1), C(1), N(1), and N(1′) is also reported and the maximum deviation is 0.010 Å for C(1), in agreement with the planarity observed for the amide group in the complex.

Mössbauer Parameters.—In agreement with their nearly regular octahedral symmetry, the complexes of Table 7 do not exhibit a measurable Mössbauer quadrupole splitting. This is also in accord with some semi-empirical IEHM calculations performed for the $[Fe(tu)_4(OH_2)_2]^{3+}$ and $[Fe(tu)_6]^{3+}$ cations, and not reported here for brevity.

All the complexes give isomer shifts of *ca.* 0.60 mm s^{-1} that are nearly temperature independent (Table 7). This suggests that the electronic and the ligand environment around the iron nucleus remain similar in all the complexes, despite the variation in the nature of the co-ordinated urea derivatives. The very small isomer-shift variation observed on going from complex (4) to (6) of Table 7 may be attributed to the substitution of two tu ligands by two water molecules in the iron co-ordination sphere. This agrees with the IEHM scheme, where a reverse order of the 4*s* electron populations has been observed on going from complex (4) to (6) of Table 7.

All the spectra exhibit a single broad Lorentzian line, whose width is *ca.* 9.5 times the natural one (0.097 mm s^{-1}).[29] The linewidth is nearly constant over the studied temperature range (see, for example, Figure 3) and seems to indicate a relaxation of spin–spin rather than spin–lattice type.[30] This behaviour is similar to that observed in $K_3[Fe(C_2O_4)_3]\cdot 2H_2O$,[31] iron(III) alum,[32] $Fe[ClO_4]_3\cdot 6H_2O$,[33] *etc.* For $[Fe(tu)_4(OH_2)_2]Cl_3\cdot 2H_2O$ in particular, the presence of electron-spin relaxation effects agrees with its Fe–Fe spacings (*ca.* 9.5 Å). The application of an external magnetic field of few kOe should reduce its Mössbauer linewidth, while low-temperature measurements should change the Lorentzian shape of its line.[34] Only experimental measurements in the presence of an external magnetic field and low-temperature techniques may confirm the nature of the relaxation, but such information is not available at present.

[9/723 *Received*, 10*th May*, 1979]

REFERENCES

[1] J. Maslowska and K. Cedzyńska, *J. Mol. Structure*, 1973, **19**, 521.

[2] B. C. Stonestreet, W. E. Bull, and R. J. Williams, *J. Inorg. Nuclear Chem.*, 1966, **28**, 1895.

[3] U. Russo, S. Calogero, N. Burriesci, and M. Petrera, *J. Inorg. Nuclear Chem.*, 1979, **41**, 25.

[3] R. J. Berni, R. R. Benerito, and H. B. Jonassen, *J. Inorg. Nuclear Chem.*, 1969, **31**, 1023.

[5] R. J. Berni, R. R. Benerito, W. M. Ayres, and H. B. Jonassen, *J. Inorg. Nuclear Chem.*, 1963, **25**, 807.

[6] A. C. T. North, D. C. Phillips, and F. S. Mathews, *Acta Cryst.*, 1968, **A24**, 351.

[7] 'International Tables for *X*-Ray Crystallography,' 2nd edn., Kynoch Press, Birmingham, 1974, vol. 4, p. 99.

[8] Ref. 7, p. 149.

[9] G. Germain, P. Main, and M. M. Woolfson, *Acta Cryst.*, 1971, **A27**, 368.

[10] W. C. Hamilton, *Acta Cryst.*, 1959, **12**, 609.

[11] A. Trautwein and F. E. Harris, *Theor. Chim. Acta*, 1973, **30**, 45.

[12] H. Basch, A. Vista, and H. B. Gray, *Theor. Chim. Acta*, 1965, **3**, 458.

[13] R. S. Mulliken, *J. Chem. Phys.*, 1955, **23**, 1833.

[14] P. Gütlich, R. Link, and A. Trautwein, 'Mössbauer Spectroscopy and Transition Metal Chemistry,' Springer–Verlag, Berlin, 1978, ch. 6.

[15] G. Sheldrick, 'SHELX 76' System of Computing Programs, University of Cambridge, 1976.

[16] J. E. Stewart, *J. Chem. Phys.*, 1957, **26**, 248.

[17] J. A. Costamagna and R. Levitus, *J. Inorg. Nuclear Chem.*, 1966, **28**, 2685.

[18] B. J. Hathaway and A. E. Underhill, *J. Chem. Soc.*, 1961, 3091.

[19] G. M. Bancroft, A. G. Maddock, W. K. Ong, and R. H. Prince, *J. Chem. Soc.* (*A*), 1966, 723.

[20] M. J. Bennett, F. A. Cotton, and D. L. Weaver, *Acta Cryst.*, 1967, **23**, 581.

[21] D. van der Helm and M. Poling, *J. Amer. Chem. Soc.*, 1976, **98**, 82.

[22] K. N. Raymond, S. S. Isied, L. D. Brown, F. R. Fronczek, and J. H. Nibert, *J. Amer. Chem. Soc.*, 1976, **98**, 1767.

[23] A. D. U. Hardy and G. A. Sim, *J.C.S. Dalton*, 1972, 2305.

[24] F. E. Mabbs, V. N. McLachlan, D. McFadden, and A. T. McPhail, *J.C.S. Dalton*, 1973, 2016.

[25] H. W. Dias and M. R. Truter, *Acta Cryst.*, 1964, **17**, 937.

[26] A. W. Pryor and P. L. Sanger, *Acta Cryst.*, 1970, **A26**, 543.

[27] C. Huiszoon and G. W. M. Tiemessen, *Acta Cryst.*, 1976, **B32**, 1604.

[28] V. M. Coiro, P. Giacomello, and E. Giglio, *Acta Cryst.*, 1971, **B27**, 2112 and refs. therein.

[29] 'Mössbauer Effect Data Index,' eds. J. G. Stevens and V. E. Stevens, Ifi–Plenum, New York, 1975, p. 54.

[30] J. W. G. Wignall, *J. Chem. Phys.*, 1966, **44**, 2462.

[31] D. Barb, L. Diamandescu, and D. Tarabasan, *J. Phys.* (*Paris*), Colloq, 6 Suppl., 1976, **C6**, 113.

[32] S. Mørup and N. Thrane, *Phys. Rev.*, 1971, **B4**, 2087.

[33] F. Sontheimer, D. L. Nagy, I. Dézsi, T. Lohner, G. Ritter, D. Seyboth, and H. Wegener, *J. Phys.* (*Paris*), Colloq. 6 Suppl., 1974, **C6**, 443.

[34] S. Mørup, in 'Mössbauer Effect Methodology,' ed. I. J. Gruverman, Plenum Press, New York, 1974, vol. IX, p. 127.